Accurate Double Many-Body Expansion Potential Energy Surface for $N_3(^4A'')$ from Correlation Scaled ab Initio Energies with Extrapolation to the Complete Basis Set Limit†

B. R. L. Galvão and A. J. C. Varandas*

Departamento de Química, Universidade de Coimbra, 3004-535 Coimbra, Portugal

Received: April 22, 2009; Revised Manuscript Received: July 15, 2009

A new global potential energy surface is reported for the $^4A''$ ground electronic state of the N_3 system from double many-body expansion theory and an extensive set of accurate ab initio energies extrapolated to the complete basis set limit. It shows three equivalent metastable potential wells for C_{2v} geometries that are separated from the three $N(^4S) + N_2$ asymptotes by energy barriers as predicted from previous ab initio work. The potential well and barrier height now predicted lie 42.9 and 45.9 kcal mol^{-1} above the atom−diatom dissociation limit, respectively, being about 1 kcal mol^{-1} lower than previous theoretical estimates. The ab initio calculations here reported predict also a $^4B_1/^4A_2$ conical intersection and reveal a new minimum with D_{3h} symmetry that lies 147 kcal mol^{-1} above the atom−diatom asymptote. All major topographical features of the potential energy surface are accurately described by the DMBE function, including the weakly bound van der Waals minima at large atom−diatom separations.

1. Introduction

The nitrogen exchange reaction has recently been the subject of considerable theoretical work since its rate constant is part of the necessary database for the design of spacecraft heat shields.[1] As experimental measurements are available only for two temperatures ($T = 1273$ and 3400 K) and have large error bars,[2–4] theoretical approaches are the only way to accurately obtain the necessary results at the temperatures achieved in the high-speed re-entry of spacecrafts into the Earth's atmosphere.

The first scattering calculations on the title system were performed on a London−Eyring−Polanyi−Sato (LEPS) potential energy surface[5] (PES), which has been for many years the only available one. Only recently, due to the inadequacy of this LEPS form of Laganà et al.[5] to describe the main features of the nitrogen atom−diatom interaction, new PESs by the same group[6,7] (denoted by the authors as L0 to L4) were proposed, with the more recent one (L4)[7] being fitted to 56 ab initio energies that were obtained using CCSD(T) (coupled-cluster singles and doubles with perturbative correction of triples) theory with the aug-cc-pVTZ basis set of Dunning[8,9] (such basis sets are generally denoted as AVXZ, where X = D, T, Q,... is the cardinal number).

The first ab initio based PES for the $N + N_2$ reaction system is due to Wang et al.,[1,10,11] who have utilized it for a quantum dynamics study of the title reaction. This PES (named WSHDSP after their authors) has employed the many-body expansion[12,13] formalism, and has been calibrated through a fit to a set of merged ab initio energies obtained using different quantum chemical treatments and basis sets.

As noted in ref 6, the thermal rate coefficients computed on the WSHDSP PES do not compare with the available experimental data as favorably as those computed on the LEPS form, which may partly be due to incompleteness of the basis set and other corrections such as incompleteness of the n-electron wave function, relativistic, and nonadiabatic corrections. Our major goal in this work will be to obtain a PES extrapolated to the complete basis set (CBS) limit, and model the energies analytically using double many-body expansion (DMBE) theory. The paper is organized as follows. Section 2 provides a description of the ab initio calculations and CBS extrapolation scheme. The modeling of the data using DMBE theory is reported in section 3, and the topological features of the PES discussed in section 4. Section 5 gathers the conclusions.

2. Ab Initio Calculations and Extrapolation Procedure

All ab initio calculations have been done with the Molpro package[14] for electronic structure calculations, and different methods tested using basis sets of the AVXZ[8,9] family (denoted for further brevity as XZ). In spite of achieving good results for regions of configuration space where one N−N bond is close to the equilibrium geometry of the N_2 molecule, the CCSD(T)[15] results do not behave correctly for $N-N_2$ cuts involving stretched diatomics, as one might expect for a single-reference based method. Conversely, the multireference configuration interaction (MRCI) approach, including the popular Davidson correction for quadruples excitations [MRCI(Q)[16,17] shows the proper behavior for the stretched structures. The CASSCF (complete active space self-consistent field) reference space for the MRCI(Q) method involves 15 correlated electrons in 12 active orbitals ($9a' + 3a''$). Unfortunately, the MRCI(Q) method is rather expensive, even using smaller basis sets, which led us to adopt a cost-effective, yet efficient, strategy whereby relatively inexpensive MRCI(Q) calculations are merged with cheap, yet accurate, CCSD(T) ones. To put them at a common level of accuracy, we have extrapolated the calculated energies to the complete basis set limit. For this, we have utilized the uniform singlet- and triplet-pair extrapolation (USTE) method proposed by one of us,[18] which shows advantages over earlier popular methodologies[19–21] and has been shown to yield accurate results even with CBS extrapolation from small basis sets. In fact, such a technique appears to provide a highly desirable route for accurately treating systems with up to a large number of electrons, as recent studies have demonstrated.[22–25] It should be further remarked that CBS extrapolation has shown[24,26] to correct largely for basis set superposition error,[27] supporting the idea

† Part of the "Vincenzo Aquilanti Festschrift".

* Corresponding author. E-mail address: varandas@qtvs1.qui.uc.pt.

10.1021/jp903719h
Published on Web 08/14/2009

that no further corrections are necessary to overcome in a simple and reasonably accurate way such an ubiquitous problem.

Aiming at a consistent description of the PES with different ab initio theories, each one chosen to be used (due to the physics of the problem or a priori design of the overall approach) at a specific region of configuration space, we suggest next a scheme to make them compatible while extrapolating to the CBS limit. As usual, at every geometry, the CBS extrapolated dynamical correlation energy is added to the CBS extrapolated CASSCF energy, yielding the total energy. First, following previous work,[18] the raw CASSCF (or simply CAS) energies are CBS extrapolated with the two-point extrapolation protocol of Karton and Martin (KM)[29] that has been originally proposed for Hartree−Fock energies:

$$E_X^{CAS}(\mathbf{R}) = E_\infty^{CAS}(\mathbf{R}) + B/X^{5.34} \tag{1}$$

where the cardinal number of the basis set is indicated in subscript (note that the CBS limit corresponds to $X = \infty$), and $\mathbf{R}$ is the collective variable of the space coordinates. For Hartree−Fock energies, this formula is known to benchmark perform with a root mean squared error of 206 μE_h or so. Such an accuracy is smaller than achieved by CBS energies obtained by extrapolating X = Q, 5, 6 energies with the exponential CBS extrapolation, and even more so when our improved CBS exponential scheme[18] is used, whereby the exponentially extrapolated energy is averaged with the raw CAS energy for X = 6. Indeed, for N_3 at the geometry corresponding to the C_{2v} minimum, the exponential-CBS and modified exponential-CBS[18] protocols predict the values of −163.434 786 and −163.434 769 E_h, which are less negative by 416 and 432 μE_h than the prediction obtained by the KM formula when applied to CAS energies. Because the error is expected to be smaller for relative energies, such an expected compensation led us to keep the method at its minimum computational complexity by avoiding the burden of having to do further calculations using two extra basis sets (X = 5, 6).

The CCSD(T) dynamical correlation energy is extrapolated with the correlation scaling/unified singlet- and triplet-pair extrapolation method based on a single pivotal geometry[30] [CS[1]/USTE(T,Q)] as follows. First, an energy is calculated with the QZ basis set at a reference geometry (any point of the set of geometries designed for the fit). Then, at this point (referred to as the pivotal geometry), the (T,Q) pair of dynamical correlation energies calculated as the difference between the CCSD(T) and CAS energies are CBS extrapolated using the USTE(T,Q)[18] protocol:

$$E_X^{dc} = E_\infty^{dc} + \frac{A_3}{(X+\alpha)^3} + \frac{A_5(0) + cA_3^{5/4}}{(X+\alpha)^5} \tag{2}$$

where $A_5(0) = 0.003\,768\,545\,9\ E_h$, $c = -1.178\,477\,13\ E_h^{-1/4}$, and $\alpha = -3/8$. The CBS extrapolated dynamical correlation energy is then added to the CBS extrapolated CAS energy to obtain the total energy at the chosen pivotal geometry. Such a strategy has indeed been shown to generate accurate functions as recently reported[25] for the ground electronic state of H_2S. It should be mentioned that the parameters employed in eq 2 are not the ones recommended[18] for CC-type methods but for the MRCI one, since the dynamical correlation (relative to the CASSCF energy, rather than the full correlation with respect to the HF energy) is being extrapolated. This may also ensure further consistency on merging the MRCI(Q) and CCSD(T) energies.

The CBS extrapolated dynamical correlation energies in the remaining CCSD(T) geometries are now obtained by correlation scaling:[28,30]

$$E_\infty^{dc}(\mathbf{R}) = \chi_{\infty,3}(\mathbf{R})\, E_3^{dc}(\mathbf{R}) \tag{3}$$

where the scaling function χ assumes the form

$$\chi_{\infty,3}(\mathbf{R}) = 1 + \frac{S_{3,2}(\mathbf{R}) - 1}{S_{3,2}(\mathbf{R}_e) - 1}[S_{\infty,3}(\mathbf{R}_e) - 1] \tag{4}$$

$\mathbf{R}_e$ is the pivotal geometry, and

$$S_{m,n}(\mathbf{R}) = \frac{E_m^{dc}(\mathbf{R})}{E_n^{dc}(\mathbf{R})} \tag{5}$$

For further details, the reader is addressed to the original papers. Suffice it to say that the reference geometry ($\mathbf{R}_e$) in the single-pivotal scheme[28] utilized here can be any point of the PES, having been taken as the geometry of the C_{2v} minimum of N_3 at the CCSD(T)/AV*T*Z level: $R_1 = R_2 = 2.39a_0$, and $\theta = 119°$.

The above extrapolation scheme can yield accurate potentials at costs as low as one may possibly ambition, its accuracy having been tested for diatomic systems through vibrational calculations. Despite the severe test of the approach, very good results have been obtained,[30] as well as for triatomic[25] and even larger systems[23,24] (these treated with a variant[33] of USTE); see also ref 34 for an application of CS to large systems.

For the CBS extrapolation of the MRCI(Q) dynamical correlation energies, we have first chosen some representative cuts, where the CCSD(T) method begins to breakdown. MRCI(Q) calculations have then been performed with DZ and TZ basis sets. To obtain a smooth merging of the CBS energies calculated from these two methods, the MRCI(Q) energies are first calibrated using the CCSD(T) ones. For this, we have utilized the CS scheme with $E_\infty^{dc}(\mathbf{R}_e)$ in eq 4 taken as the extrapolated CCSD(T) value obtained above. Such a procedure requires explicit MRCI(Q) calculations only for DZ and TZ basis sets while ensuring that both methods yield identical CBS energies at the pivotal geometry: $E_\infty^{dc}(\text{MRCI(Q)},\mathbf{R}_e) = E_\infty^{dc}(\text{CCSD(T)},\mathbf{R}_e)$. An illustrative cut is presented in Figure 1, where the pivotal geometry has been chosen so as to warrant that CCSD(T) theory provides good results. Note that the scaling function in eq 4 imposes that the extrapolated MRCI(Q) and CCSD(T) energies coincide at $R_e = 3.3a_0$. Thus, no discontinuity arises in the energy along the chosen cut.

3. DMBE Potential Energy Surface

Within the DMBE[31,32,35,36] framework, the potential energy surface is first written as a sum of one-, two-, and three-body terms:

$$V(R_1,R_2,R_3) = V^{(1)} + \sum_{i=1}^{3} V^{(2)}(R_i) + V^{(3)}(R_1,R_2,R_3) \tag{6}$$

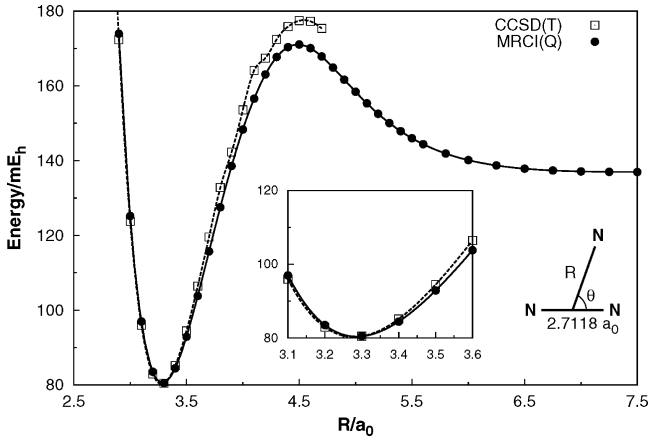

Figure 1. Extrapolated CCSD(T) and MRCI(Q) energies used to calibrate the DMBE PES for a cut corresponding to a N atom approaching N_2 with $R_{NN} = 2.7118a_0$ and the Jacobi angle fixed at 30°. In this and all subsequent plots, the zero of energy corresponds to the N_2 + N reaction channel (with the diatomic in its equilibrium geometry), as described by extrapolated CCSD(T) energies.

To fix the zero of the energy of the PES at a N_2 molecule at equilibrium and one N(^{4}S) atom infinitely separated, we impose that the one-body term equals to $V^{(1)} = -2D_e$, where D_e is the well depth of the N_2 molecule. Clearly, the PES ensures the proper asymptotic limits, i.e., $V(R_e,\infty,\infty) = 0$, and $V(\infty,\infty,\infty) = D_e$. Each n-body term is now split into extended Hartree−Fock [$V^{(n)}_{EHF}$] and dynamical correlation [$V^{(n)}_{dc}$] contributions, whose analytical forms are described in detail in the following sections. Although all such forms have a semiempirical motivation from past work, it should be stressed that they are here utilized to fit the CBS extrapolated data, and hence the resulting PES contains no information at all that is alien to the ab initio methods that have been utilized.

3.1. Two-Body Energy Terms. The diatomic potential curve for the ground state of molecular nitrogen has been modeled using the extended Hartree−Fock approximate correlation energy method for diatomic molecules, including the united-atom limit (EHFACE2U),[37] and fitted to CBS extrapolated energies described in the previous section for the asymptotic atom−diatom cuts. The EHF term assumes the form

$$V^{(2)}_{EHF}(R) = -\frac{D}{R}(1 + \sum_{i=1}^{n} a_i r^i)\exp[-\gamma(r)r] \qquad (7)$$

where $r = R - R_e$ is the displacement from the equilibrium diatomic geometry, D and a_i ($i = 1,..., n$) are adjustable parameters, and the range decaying term in the exponential is given by form $\gamma(r) = \gamma_0[1 + \gamma_1 \tanh(\gamma_2 r)]$.

In turn, the dynamical correlation part assumes the form

$$V^{(2)}_{dc}(R) = -\sum_{n=6,8,10,...} C_n \chi_n(R) R^{-n} \qquad (8)$$

where

$$\chi_n(R) = \left[1 - \exp\left(-A_n\frac{R}{\rho} - B_n\frac{R^2}{\rho^2}\right)\right]^n \qquad (9)$$

is a charge-overlap damping function for the long-range dispersion energy, and the summation in eq 8 is truncated at $n = 10$. In turn, $A_n = \alpha_0 n^{-\alpha_1}$ and $B_n = \beta_0 \exp(-\beta_1 n)$ are auxiliary functions,[31,35] with $\alpha_0 = 16.366\,06$, $\alpha_1 = 0.701\,72$, $\beta_0 = 17.193\,38$, and $\beta_1 = 0.095\,74$ being universal-type parameters. Moreover, $\rho = 5.5 + 1.25R_0$ is a scaling parameter, $R_0 = 2(\langle r_A^2\rangle^{1/2} + \langle r_B^2\rangle^{1/2})$ is the Le Roy[38] parameter for the onset of the undamped R^{-n} expansion, and $\langle r_X^2\rangle$ is the expectation value of the squared radius for the outermost electrons of atom X. All coefficients used in the $N_2(X^1\Sigma_g^+)$ potential curve, and other parameters necessary to construct the DMBE function are given as Supporting Information.

3.2. Three-Body Energy Terms. ***3.2.1. Three-Body Dynamical Correlation Energy.*** The three-body dynamical correlation energy term assumes the form[39]

$$V^{(3)}_{dc} = -\sum_i \sum_n f_i(\mathbf{R})\, C_n^{(i)}(R_i,\theta_i)\, \chi_n(r_i) r_i^{-n} \qquad (10)$$

where R_i, r_i, and θ_i are the Jacobi coordinates (R_i is a NN distance, r_i the N−NN corresponding separation, and θ_i the included angle), and $f_i = {}^1/_2\{1 - \tanh[\xi(\eta R_i - R_j - R_k)]\}$ is a switching function with parameters fixed at $\eta = 6$ and $\xi = 1a_0^{-1}$; corresponding expressions hold for R_j, R_k, f_j, and f_k. Regarding the damping function $\chi_n(r_i)$, we still adopt eq 9 but with R_i replaced by r_i, and R_0 estimated as for the Si−N diatomic (Si corresponds to the united atom of the coalesced N_2 diatom; see ref 39).

The atom−diatom dispersion coefficients in eq 10 also assume their usual form

$$C_n^{(i)}(R_i,\theta_i) = \sum_L C_n^L(R) P_L(\cos\theta_i) \qquad (11)$$

where $P_L(\cos\theta_i)$ denotes the Lth Legendre polynomial. The expansion in eq 11 has been truncated by considering only the coefficients C_6^0, C_6^2, C_8^0, C_8^2, C_8^4, C_{10}^0; all other coefficients have been assumed to make negligible contributions. To estimate the dispersion coefficients, we have utilized the generalized Slater−Kirkwood approximation,[40] with the dipolar polarizabilities calculated at the MRCI/AVQZ level. The atom−diatom dispersion coefficients so calculated for a set of internuclear distances have then been fitted to the functional form

$$C_n^{L,N_1-N_2N_3}(R) = C_n^{L,N_1N_2} + C_n^{L,N_1N_3} + D_M(1 + \sum_{i=1}^{3} a_i r^i)\exp(-\sum_{i=1}^{3} b_i r^i) \qquad (12)$$

where $b_1 = a_1$, and $C_n^{L,NN}$ is the atom−atom dispersion coefficient for $L = 0$ and zero for other values of L. The internuclear dependence of such coefficients are displayed in Figure 2. As noted elsewhere,[39] eq 10 causes an overestimation of the dynamical correlation energy at the atom−diatom dissociation channels. This can be corrected by multiplying the two-body dynamical correlation energy for the ith pair by $\Pi_{j\neq i}(1 - f_j)$, where f_i is the switching function used in $V^{(3)}_{dc}$ term, with corresponding expressions for channels j and k.

3.2.2. Three-Body Extended Hartree−Fock Energy. With the one- and two-body terms and also the three-body dynamical correlation energy at hand, the three-body EHF term can now be determined for every geometry by subtracting the other contributions:

$$V_{\mathrm{EHF}}^{(3)}(\mathbf{R}) = E(\mathbf{R}) - V_{\mathrm{dc}}^{(3)}(\mathbf{R}) - \sum_{i=1}^{3} V^{(2)}(R_i) + 2D_{\mathrm{e}} \tag{13}$$

Of course, the representation of the PES must be symmetric with respect to permutation of the coordinates. Such a requirement is satisfied by using the integrity basis:

$$\Gamma_1 = Q_1 \tag{14}$$

$$\Gamma_2 = {Q_2}^2 + {Q_3}^2 \tag{15}$$

$$\Gamma_3 = Q_3({Q_3}^2 - 3{Q_2}^2) \tag{16}$$

where Q_i are symmetry coordinates.[12,13,41] The functions Γ_i are all totally symmetric in the three-particle permutation group S_3. Thus, any polynomial built from Γ_i also transforms as the totally symmetric representation of S_3. The EHF three-body energy is then fitted to a function in these coordinates using a three-body distributed polynomial[42] approach:

$$V_{\mathrm{EHF}}^{(3)}(\mathbf{R}) = \sum_{m=1}^{4} P^{(m)} T^{(m)}(\mathbf{R}) \tag{17}$$

where the polynomials are defined as

$$P^{(m)} = \sum_{i,j,k} c_{ijk}^{(m)} \Gamma_1^i \Gamma_2^j \Gamma_3^k \tag{18}$$

and $T(\mathbf{R})$ is a range-determining factor that ensures that the three-body term vanishes at large interatomic distances,

$$T^{(m)}(\mathbf{R}) = \prod_{j=1}^{3} \{1 - \tanh[\gamma^{(m)}(R_j - R_0^{(m)})]\} \tag{19}$$

To describe the van der Waals region, a polynomial with the range function above is not suitable since it vanishes with a similar decay rate for all bond distances. To overcome such a difficulty, we have chosen one bond length to have a different reference value and decaying parameter (thus having C_{2v} symmetry). Since this cannot impose the correct permutational symmetry, a summation of three such functions has been utilized. The $V_{\mathrm{EHF}}^{(3)}$ function defined above contains a total of 276 linear parameters (c_{ijk}^{m}, as given in the Supporting Information) that have been calibrated using a total of 1592 ab initio points. A summary of the errors in the fitting procedure is displayed in stratified form in Table 1. It should be pointed out that larger weights were attributed to the most important regions of the PES, namely stationary points (in particular for the subtle van der Waals minima).

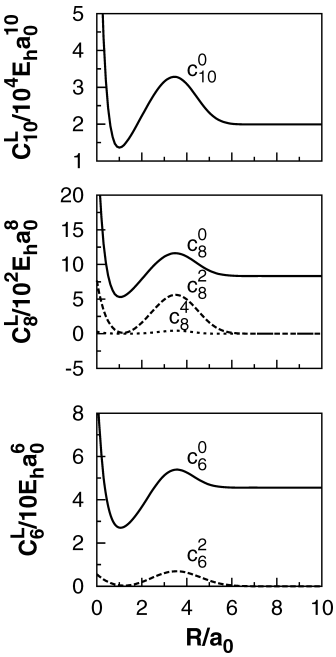

Figure 2. Dispersion coefficients for the atom−diatom asymptotic channel as a function of the diatomic internuclear distance.

4. Features of DMBE Potential Energy Surface

Table 2 compares the attributes of the two main stationary points of the DMBE form with the corresponding attributes from other potential energy surfaces.[1,7] Also included are the values calculated at CCSD(T)/AVTZ and CCSD(T)/CBS level. As can be seen, the extrapolation of the ab initio energies to the CBS limit leads to a significant decrease in the height of the well and transition state relative to the atom−diatom limit, being predicted respectively as 42.9 and 45.9 kcal mol^{-1}. The energy difference between them is also increased by ~0.6 kcal mol^{-1}, while their geometries are essentially indistinguishable from the raw CCSD(T) ones at the TZ level.

The calculated MRCI(Q) energies (performed just for the ground state) here reported show also a shallow D_{3h} minimum surrounded by two C_{2v} stationary structures, a feature that appears to arise due to a conical intersection between the ground and first excited state of $^4A''$ symmetry, or between the $^4B_1$ and $^4A_2$ states in C_{2v} symmetry, as shown in Figure 3, where single state CASSCF calculations performed for each symmetry are shown. Indeed, as demonstrated in the insert of Figure 3, the wave function changes sign when transported adiabatically along a closed path encircling the point of crossing (with a small radius of $0.6a_0$ to avoid encircling more than one crossing), as it should by the Longuet−Higgins'[43] sign change theorems for a conical intersection. Note that the sign change has been illustrated by plotting the dominant component of the CAS vector along the chosen path, following pioneering work for the LiNaK system.[44]

A full view of the DMBE PES for C_{2v} insertion of a nitrogen atom in the nitrogen diatomic is shown at Figure 4 where the two saddle points and minimum described above are apparent. To improve the representation of this region of the PES, a relatively dense grid of MRCI(Q) points has been calculated and used in the fit. As shown, the DMBE function predicts a D_{3h} minimum with a characteristic bond length of $2.95a_0$, which lies 146.6 kcal mol^{-1} above the N + N_2 reaction asymptote (but still below the energy for the three separated-atoms limit). Such a minimum is connected to the absolute ones by saddle points in the C_s ground state), being the full numerical characterization (geometries, energies, and harmonic vibrational frequencies) of these stationary points reported in Table 3.

TABLE 1: Stratified Global Root-Mean-Square Deviations (in kcal mol^{-1}) of $N_3(^4A'')$ DMBE Potential Energy Surface

energy[a]	N^b	rmsd
0	85	0.001
10	279	0.212
20	335	0.281
30	369	0.358
40	408	0.402
50	704	0.380
60	819	0.451
70	899	0.543
80	971	0.615
90	1017	0.625
100	1073	0.673
250	1443	0.908
500	1528	0.952
1000	1564	0.963
3000	1585	0.979

[a] In kcal mol^{-1} and relative to the N(^{4}S) + N_2 asymptote. [b] Number of calculated ab initio points up to the indicated energy range.

TABLE 2: Stationary Points of $N_3(^4A'')$ Potential Energy Surface, for Different Fitted Forms and CCSD(T) ab Initio Values (at AVTZ and CBS Levels)[a]

feature	property	WSHDSP[b]	L4[c]	AVTZ[d]	CBS	DMBE
Min (C_{2v})	R_1/a_0	2.40	2.40	2.39	2.38	2.38
	R_2/a_0	2.40	2.40	2.39	2.38	2.38
	θ/deg	120	119	119	119	119
	ΔE^e	43.7	44.5	44.7	42.9	42.9
	ω_1/cm^{-1}		860			702
	ω_2/cm^{-1}		1279			1323
	ω_3/cm^{-1}		665			566
sp (C_s)	R_1/a_0	2.23	2.24	2.22	2.20	2.20
	R_2/a_0	2.80	2.77	2.84	2.85	2.83
	θ/deg	119	117	117	117	116
	ΔE^e	47.2	47.4	47.1	45.9	45.9
	ω_1/cm^{-1}		599			511
	ω_2/cm^{-1}		760i			652i
	ω_3/cm^{-1}		1585			1740

[a] The geometries are in valence coordinates. [b] From ref 1. [c] The geometry optimizations with the L4 potential energy surface[7] are from the present work. [d] Ab initio geometry optimization at the CCSD(T)/AVTZ level. [e] In kcal mol^{-1}, relative to the N(^{4}S) + N_2 asymptote.

All major features of the PES are probably better viewed in the relaxed triangular plot[45] of Figure 5 utilizing scaled hyperspherical coordinates ($\beta^\star = \beta/Q$ and $\gamma^\star = \gamma/Q$):

$$\begin{pmatrix} Q \\ \beta \\ \gamma \end{pmatrix} = \begin{pmatrix} 1 & 1 & 1 \\ 0 & \sqrt{3} & -\sqrt{3} \\ 2 & -1 & -1 \end{pmatrix} \begin{pmatrix} R_1^2 \\ R_2^2 \\ R_3^2 \end{pmatrix} \tag{20}$$

Note that the perimeter of the molecule is relaxed such that the energy of the triangle formed by the three atoms is lowest at any point. Clearly visible are the equivalent stationary structures for the N + N_2 exchange reaction (wells and transition states), as well as those in the vicinity of the D_{3h} geometry ($\gamma^\star = \beta^\star = 0$) already commented.

The equivalent N−N_2 van der Waals minima are described with a root mean squared deviation of ~0.001 kcal mol^{-1} for the 144 ab initio energies shown in Figure 6. Note that there are two types of such minima, one for geometries with

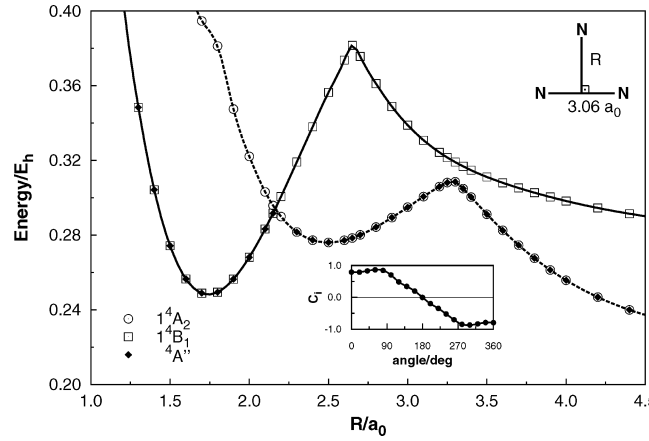

Figure 3. CASSCF description of the conical intersection with the AVTZ basis set. The open symbols connected by smooth splines correspond to points calculated in the $^4A_2$ and $^4B_1$ states of C_{2v} symmetry, while the solid diamonds correspond to calculations with $^4A''$ symmetry (the zero of energy is the CASSCF value for the N(^{4}S) + N_2 channel). Shown in the inset is an illustration of the sign change theorem for a closed path (circle) around the conical intersection (the point of crossing shown in the main plot): c_i is the coefficient of the dominant configuration in the CASSCF wave function of the first $^4A''$ state.

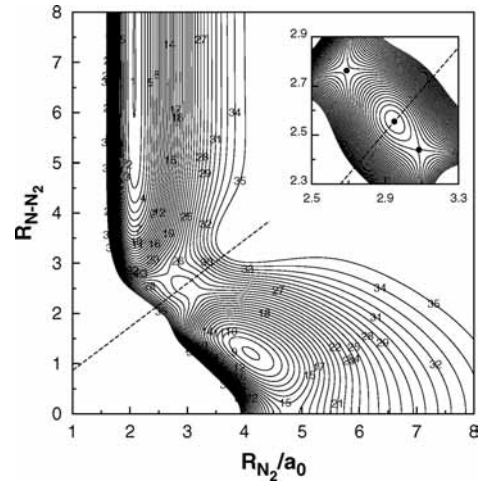

Figure 4. Contours plot for the C_{2v} insertion of the N atom into N_2. Contours are equally spaced by 10 mE_h, starting at zero. The dashed line shows the location of D_{3h} geometries while the inset displays a zoom around the D_{3h} minima (contours spaced by 0.5 mE_h), with the stationary points indicated by filled circles.

C_{2v} symmetry, and the other for geometries with $C_{\infty v}$ symmetry, the deepest being T-shaped like.

The isotropic and leading anisotropic terms in a Legendre expansion of the N−N_2 interaction potential are important quantities for the study of scattering processes, with the sign of V_2 indicating whether or not the molecule prefers to orient its axis along the direction of the incoming atom: a negative value favors the collinear approach while a positive value favors the approach through C_{2v} geometries. Such potentials are shown in Figure 7. Note that the well and barrier in the short-range region of the leading anisotropic component, V_2, correspond to the C_{2v} well and C_s transition state, while the negative values attained by both the isotropic and anisotropic components at distances larger than 6 a_0 reflect the attractive nature of the van der Walls interaction.

TABLE 3: D_{3h} Minimum and Nearby Stationary Features Arising from Approximating Conical Intersection with Single-Sheeted DMBE Formalism[a]

	Min (D_{3h})	sp_1[b] (C_{2v})	sp_2 (C_{2v})
R_1/a_0	2.95	2.69	3.08
R_2/a_0	2.95	3.07	2.89
R_3/a_0	2.95	3.07	2.89
ΔE[c]	146.6	151	147.5
ω_1/cm^{-1}	1278	1258i	1271
ω_2/cm^{-1}	855	1233i	964i
ω_3/cm^{-1}	855	1209	1020

[a] See the text. [b] Saddle point with two imaginary frequencies. [c] In kcal mol^{-1}, relative to the $N(^4S) + N_2$ asymptote.

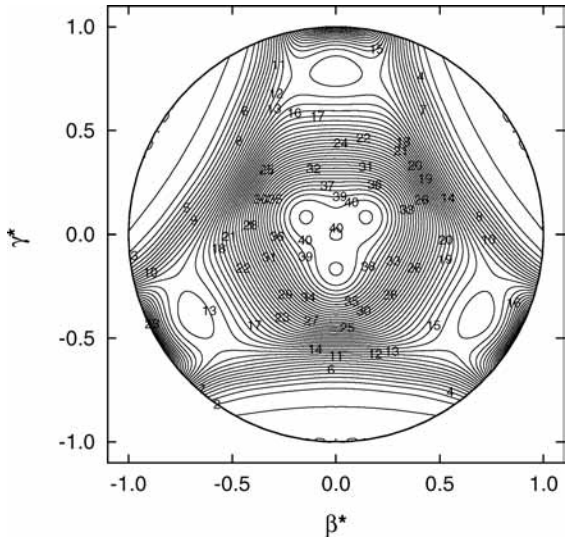

Figure 5. Relaxed triangular plot of the hypersurface. Contours are equally spaced by 6 mE_h, starting at zero.

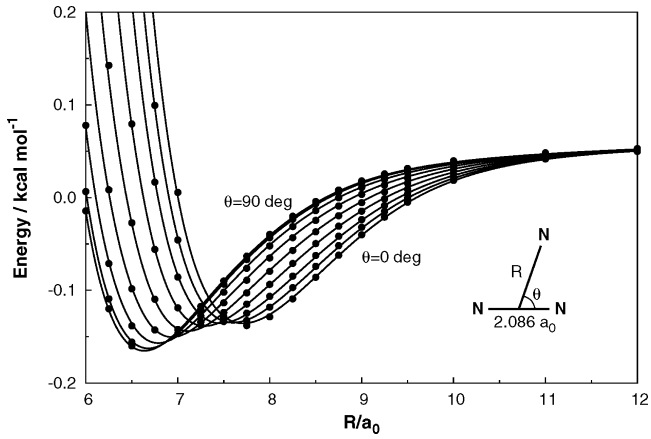

Figure 6. Cuts of DMBE potential energy surface along the atom−diatom radial coordinate for a fixed diatomic bond distance of $2.086a_0$ at the van der Waals region for several angles of insertion. The solid points are the extrapolated CCSD(T) while the lines corresponds to the fitted surface.

Finally, we report the results of a preliminary dynamics study aiming at testing the DMBE potential energy surface here reported. Specifically, we have run trajectories for the exchange reaction $N + N_2 \rightarrow N_2 + N$ using the quasiclassical trajectory method as implemented in the Venus computer code.[46] The rate constants here reported have been calculated directly using Maxwell−Boltzmann distributions for the translational energy and rovibrational quantum states.[47] Due to the high barrier of the exchange reaction ($E_0 = 45.9$ kcal mol^{-1}, including the zero-point energies of the reactants and transition state), all trajectories with internal energy below E_0 were not integrated and simply considered as nonreactive.[48] A total of 6.4×10^5 trajectories has been run for each temperature, with the impact parameter being $b_{max} = 1.8$ Å (determined as usual by a trial and error procedure). Table 4 compares the thermal rate coefficients so calculated at two temperatures with the results obtained from other potential energy surfaces. The results for the DMBE and L4 PESs have been calculated using our own QCT approach for a better comparison, while those of WSHDSP utilized the quantal J−K-shifting method. As expected from the smaller barrier in the DMBE function, a larger reactivity is predicted than with other available forms, pointing to a slightly better agreement with the available experimental data.

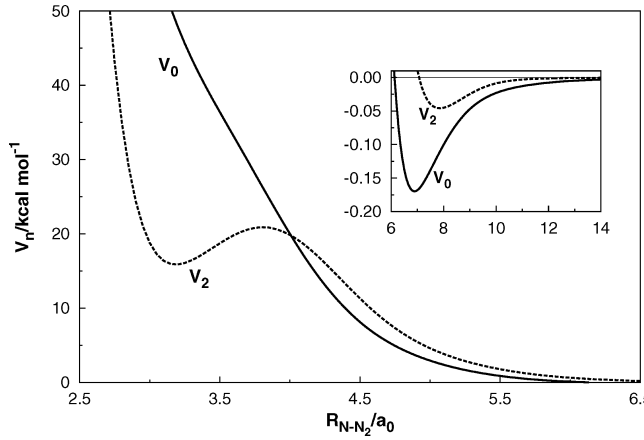

Figure 7. Isotropic (V_0) and leading anisotropic (V_2) components of the N−N_2 interaction potential, with the diatomic fixed at the equilibrium geometry.

TABLE 4: Logarithm of the Thermal Rate Coefficient (in cm^3s^{-1}) for the $N + N_2$ Exchange Reaction

temp (K)	DMBE[a]	L4[a]	WSHDSP[b]	exp
1273	−18.4	−18.7	−18.5	≤−16.9[c]
3400	−12.9	−13.0	−13.0	−12.3 ± 1.0[d]

[a] From QCT calculations carried out in the present work. [b] Reference 6. [c] Reference 3. [d] Reference 4.

5. Conclusions

We have reported a single-sheeted DMBE potential energy surface for the quartet state of N_3 based on a fit to CBS extrapolated CCSD(T) and MRCI(Q) energies. A procedure of the smooth merger of these two correlated methods at the CBS-limit has been developed to calculate the points on the single potential energy surface based on the modified correlation scaling (CS)-scheme which assures that there exist no discontinuities. The MRCI(Q)/CBS energies are calibrated using the CCSD(T)/CBS result at the pivotal geometry (e.g., local minimum). In fact, the procedure is formulated in such a way that at the reference pivotal geometry of N_3 the MRCI(Q)/CBS energy coincides exactly with the CCSD(T)/CBS energy. The DMBE potential energy surface describes accurately all topographical features of the calculated ab initio energies, except for the conical intersections that have been replaced by narrowly avoided ones. As an asset of DMBE theory, the van der Waals regions are also described accurately. Finally, exploratory quasiclassical trajectories on the atom−diatom nitrogen reaction have shown that the PES is suitable for any kind of dynamics studies. A detailed report of such studies is planned for a future publication.

Acknowledgment. This work has the support of European Space Agency under ESTEC Contract No. 21790-/08/NL/HE, and Fundação para a Ciência e Tecnologia, Portugal (contracts POCI-/QUI/60501/2004, POCI/AMB/60261/2004) under the auspices of POCI 2010 of Quadro Comunitário de Apoio III cofinanced by FEDER.

Supporting Information Available: All coefficients necessary to construct the potential energy surface here reported. This material is available free of charge via the Internet at http://pubs.acs.org.

References and Notes

(1) Wang, D.; Stallcop, J. R.; Huo, W. M.; Dateo, C. E.; Schwenke, D. W.; Partridge, H. *J. Chem. Phys.* **2003**, *118*, 2186.
(2) Back, R. A.; Mui, J. Y. P. *J. Phys. Chem.* **1962**, *66*, 1362.
(3) Bar-Nun, A.; Lifshitz, A. *J. Chem. Phys.* **1967**, *47*, 2878.
(4) Lyon, R. K. *Can. J. Chem.* **1972**, *50*, 1437.
(5) Laganà, A.; Garcia, E.; Ciccarelli, L. *J. Phys. Chem.* **1987**, *91*, 312.
(6) Garcia, E.; Saracibar, A.; Laganà, A.; Skouteris, D. *J. Phys. Chem. A* **2007**, *111*, 10362.
(7) Garcia, E.; Saracibar, A.; Gomez-Carrasco, S.; Laganà, A. *Phys. Chem. Chem. Phys.* **2008**, *10*, 2552.
(8) Dunning, T. H., Jr. *J. Chem. Phys.* **1989**, *90*, 1007.
(9) Kendall, R. A.; Dunning, T. H., Jr.; Harrison, R. J. *J. Chem. Phys.* **1992**, *96*, 6769.
(10) Wang, D.; Huo, W. M.; Dateo, C. E.; Schwenke, D. W.; Stallcop, J. R. *Chem. Phys. Lett.* **2003**, *379*, 132.
(11) Wang, D.; Huo, W. M.; Dateo, C. E.; Schwenke, D. W.; Stallcop, J. R. *J. Chem. Phys.* **2004**, *120*, 6041.
(12) Varandas, A. J. C.; Murrell, J. N. *Faraday Discuss. Chem. Soc.* **1977**, *62*, 92.
(13) Murrell, J. N.; Carter, S.; Farantos, S. C.; Huxley, P.; Varandas, A. J. C. *Molecular Potential Energy Functions*; Wiley: Chichester, U.K., 1984.
(14) Werner H. J. Knowles, P. J. *MOLPRO is a package of ab initio programs*; Almlöf, J., Amos, R. D. , Deegan, M. J. O., Elbert, S. T., Hampel, C., Meyer, W., Peterson, K. A., Pitzer, R., Stone, A. J., Taylor, P. R., Lindh. R., contributors; 1998.
(15) Watts, J. D.; Gauss, J.; Bartlett, R. J. *J. Chem. Phys.* **1993**, *98*, 8718.
(16) Werner, H. J.; Knowles, P. J. *J. Chem. Phys.* **1988**, *89*, 5803.
(17) Knowles, P. J.; Werner, H. J. *Chem. Phys. Lett.* **1988**, *145*, 514.
(18) Varandas, A. J. C. *J. Chem. Phys.* **2007**, *126*, 244105.
(19) Helgaker, T.; Klopper, W.; Koch, H.; Noga, J. *J. Chem. Phys.* **1997**, *106*, 9639.
(20) Truhlar, D. G. *Chem. Phys. Lett.* **1998**, *294*, 45.
(21) Varandas, A. J. C. *J. Chem. Phys.* **2000**, *113*, 8880.
(22) Varandas, A. J. C. *J. Chem. Phys.* **2008**, *129*, 234103.
(23) Varandas, A. J. C. *Chem. Phys. Lett.* **2008**, *463*, 225.
(24) Varandas, A. J. C. *J. Comput. Chem.* **2009**, *30*, 379.
(25) Song, Y. Z.; Varandas, A. J. C. *J. Chem. Phys.* **2009**, *130*, 134317.
(26) Varandas, A. J. C. *Theor. Chem. Acc.* **2008**, *119*, 511.
(27) Boys, F.; Bernardi, F. *Mol. Phys.* **1970**, *19*, 553.
(28) Varandas, A. J. C.; Piecuch, P. *Chem. Phys. Lett.* **2006**, *430*, 448.
(29) Karton, A.; Martin, J. M. L. *Theor. Chem. Acc.* **2006**, *115*, 330.
(30) Varandas, A. J. C. *Chem. Phys. Lett.* **2007**, *443*, 398.
(31) Varandas, A. J. C. *Adv. Chem. Phys.* **1988**, *74*, 255.
(32) Varandas, A. J. C. *Advanced Series in Physical Chemistry*; World Scientific Publishing: Singapore, 2004; Chapter *5*, p 91.
(33) Varandas, A. J. C. *J. Phys. Chem. A* **2008**, *112*, 1841.
(34) Lutz, J. J.; Piecuch, P. *J. Chem. Phys.* **2008**, *128*, 154116.
(35) Varandas, A. J. C. *J. Mol. Struct. (THEOCHEM)* **1985**, *21*, 401.
(36) Varandas, A. J. C. *Lecture Notes in Chemistry*; Laganà, A., Riganelli, A., Eds.; Springer: Berlin, 2000; Vol. 75, p 33.
(37) Varandas, A. J. C.; Silva, J. D. *J. Chem. Soc., Faraday Trans.* **1992**, *88*, 941.
(38) Le Roy, R. J. *Spec. Period. Rep. Chem. Soc. Mol. Spectrosc.* **1973**, *1*, 113.
(39) Varandas, A. J. C. *J. Chem. Phys.* **1996**, *105*, 3524.
(40) Matías, M. A.; Varandas, A. J. C. *Mol. Phys.* **1990**, *70*, 623.
(41) Murrell, J. N.; Sorbie, K. S.; Varandas, A. J. C. *Mol. Phys.* **1976**, *32*, 1359.
(42) Martínez-Núñez, E.; Varandas, A. J. C. *J. Phys. Chem. A* **2001**, *105*, 5923.
(43) Longuet-Higgins, H. C. *Proc. R. Soc. Ser. A* **1975**, *344*, 147.
(44) Varandas, A. J. C.; Tennyson, J.; Murrell, J. N. *Chem. Phys. Lett.* **1979**, *61*, 431.
(45) Varandas, A. J. C. *Chem. Phys. Lett.* **1987**, *138*, 455.
(46) Hase, W. L.; Duchovic, R. J.; Hu, X.; Komornicki, A.; Lim, K. F.; Lu, D.; Peslherbe, G. H.; Swamy, K. N.; Linde, S. R. V.; Varandas, A. J. C.; Wang, H.; Wolf, R. J. *QCPE Bull.* **1996**, *16*, 43.
(47) Caridade, P. J. S. B.; Varandas, A. J. C. *J. Phys. Chem. A* **2004**, *108*, 3556.
(48) Varandas, A. J. C.; Caridade, P. J. S. B.; Zhang, J. Z. H.; Cui, Q.; Han, K. L. *J. Chem. Phys.* **2006**, *125*, 064312.

JP903719H